

Molecular Dynamics Simulation of Hydrogen Fluoride Mixtures with 1-Ethyl-3-methylimidazolium Fluoride: A Simple Model for the Study of Structural Features[†]

M. Salanne, C. Simon,* and P. Turq

Laboratoire Liquides Ioniques et Interfaces Chargées (UMR 7612 UPMC-CNRS-ESPCI),
Université P. et M. Curie, 4 place Jussieu, 75252 Paris Cedex 05, France

Received: July 13, 2005; In Final Form: October 20, 2005

Mixtures of hydrogen fluoride with ionic liquids show unique physicochemical properties, including their ability to form polyfluoride species (pointed out for the first time in this media by von Rosenvinge et al. *J. Chem. Phys.* **1997**, 107, 8012). Among those systems the acidic 1-ethyl-3-methylimidazolium fluoride (EMIF•2.3HF) has been widely studied experimentally since it is the more promising for electrochemical applications. Recent studies (Hagiwara et al. *J. Electrochem. Soc.* **2002**, 149, D1), while yielding many results, raised some questions about structural features of the liquid: absence of hydrogen bonds between the EMI⁺ ring hydrogen atoms and the fluoride anions, persistence of stacks and layers of cations similar to those existing in the crystal, and interpretation of the X-ray diffraction spectra. To address these questions, we have developed a simple molecular dynamics model. Our simulations are very consistent with experimental results and complete them, providing an atomic scale interpretation.

1. Introduction

Room-temperature ionic liquids, RTILs, based on alkylimidazolium cations build up an interesting family of products. Their features are chemical and thermal stability, nonvolatility, high ionic conductivity, and a wide electrochemical potential window. Consequently they are considered as a promising solvent class for chemistry and electrochemistry.

Recently, a new RTIL has been synthesized, the acidic 1-ethyl-3-methylimidazolium fluoride (EMIF•2.3HF),¹ which shows unique properties. First, this compound possesses a high electrical conductivity² of 100 mS cm⁻¹ and a low viscosity of 4.85 cP. Practical applications as an electrolyte are therefore considered for many fields in electrochemistry.^{3,4} Second, studies have shown that this ionic liquid was a good fluoride ion source with easy handling for organic chemistry. It has already been successfully used for fluorination of epoxides⁵ and alkenes.⁶

Moreover, the EMIF•2.3HF mixture is of particular interest from a theoretical point of view. It is indeed an intermediate between molten salts and molecular liquids. This particularity relates this system to the potassium fluoride solution in hydrogen fluoride, KF•2HF, which is industrially used for electrochemical generation of fluorine. This liquid has already been studied by molecular dynamics,^{7–9} but very few experimental data are available due to its corrosivity. As EMIF•2.3HF is quite easier to handle, its structural and dynamical properties are extensively investigated;¹⁰ therefore this system provides a good reference to which we can confront molecular dynamics simulations results.

On the molecular scale, one of the main characteristics of ionic liquids containing HF molecules is their ability to form polyfluoride species. Although it was proved that H_nF_{n+1}⁻ anions exist for *n* = 1, 2, 3, and 4 in the KF•*x*HF crystals (for

x = 1, 2, 2.5, 3, and 4), their existence in the liquid phase could only be determined recently by IR spectroscopy in tetraalkylammonium¹¹ and dialkylimidazolium¹² fluorohydrogenates. As *ab initio*⁷ and classical⁸ molecular dynamics simulations were able to predict the existence of those polyfluorides, these techniques should be useful to determine their properties and to correlate them to the physicochemical behaviors of the ionic liquids containing them.

As will be shown in the following sections, it is possible to use very classical models for fluoride and imidazolium ions and for pure hydrogen fluoride to build a good model for the liquid EMIF•2.3HF. The obtained structure agrees very well with X-ray diffraction data available and allows a deeper and renewed interpretation of experimental data. Formation of polyfluoride species was observed, and their structural and vibrational properties are in agreement with *ab initio* molecular dynamics results.

2. Model and Methods

2.1. Interaction Potentials. In our simulations we considered three distinct types of molecules: 1-Ethyl-3-methylimidazolium cations and fluoride anions are the charge-carrying species whereas the HF molecules are globally neutral. In this section we will first focus on the models for hydrogen fluoride and imidazolium cations, i.e., intramolecular and intermolecular interaction between molecules of the same kind, then we will present the intermolecular potentials used between molecules of a different type, i.e., the mixing rules.

2.1.1. Hydrogen Fluoride. Many valuable potentials have been developed for representation of pure HF. These models, which give good results on the thermodynamics and dynamics of the liquid state, can be distinguished into two groups: the models describing HF as rigid and the central force potentials.

To decide which category to use we considered the following arguments. Absence of fluoride anions in our system is the first

[†] Part of the special issue "Michael L. Klein Festschrift".

* Author to whom correspondence should be addressed. Phone: 33-1-44-27-32-65. Fax: 33-1-44-27-32-28. E-mail: csimon@ccr.jussieu.fr.

one. The principal interest of central force potentials is to allow the splitting of HF into a pair of ions to mimic self-ionization. Fluoride anion is indeed the conjugated basis of HF, and the self-ionization constant of HF molecules in pure liquid HF is of $10^{-12.5}$ at 273 K. Since simulation cells are limited to a few thousand atoms, the probability to observe dissociated free proton is negligible. There is therefore a priori no interest in using a central force model rather than a rigid one. On the basis of previous successful studies on KF•2HF, we chose the so-called HF3 model developed by Klein et al.¹³ This model is a three-site one in which the bond length is 0.9118 Å. The fluorine and hydrogen atoms carry charges of $+0.68e$, and a $-1.36e$ compensating charge is placed along the line joining the two atoms at a distance of 0.165 Å from the fluorine atom. This correctly depicts the various multipole moments of the isolated molecule. It also describes explicitly, through a Morse potential, the hydrogen bond between molecules, which is responsible for the formation of oligomers in pure HF. This bond has also very similar properties with the bond between fluoride and HF in polyfluorides. The non-Coulombic terms of the intermolecular potential between two molecules are of the following form (where all the potentials are expressed in kcal mol⁻¹ and distances in Å)

$$V_{\text{FF}}(r) = 2 \times 10^5 \exp(-4.25r) - V^{\text{DISP}} \quad (1)$$

$$V_{\text{FH}}(r) = 2(\exp(-10.6(r - 1.6)) - 2 \exp(-5.3(r - 1.6))) \quad (2)$$

$$V_{\text{HH}}(r) = 600 \exp(-3.34r) \quad (3)$$

$$V^{\text{DISP}} = f(r) \left(\frac{220}{r^6} + \frac{400}{r^8} + \frac{4500}{r^{10}} \right) \quad (4)$$

$$f(r) = \exp\left(-\left(\frac{4.7}{r} - 1\right)^2\right) \quad \text{if } r \leq 4.7 \quad (5)$$

$$= 1 \quad \text{else}$$

2.1.2. Imidazolium Cations. We used the AMBER force field,¹⁴ developed by Cornell et al., to model imidazolium molecules. In this representation, the potential energy takes the following form

$$V_{\text{total}} = \sum_{\text{bonds}} K_r(r - r_{\text{eq}})^2 + \sum_{\text{angles}} K_\theta(\theta - \theta_{\text{eq}})^2 + \sum_{\text{dihedrals}} \frac{V_n}{2} [1 + \cos(n\phi - \gamma)] + \sum_{i < j} \left[\frac{A_{ij}}{r_{ij}^{12}} - \frac{B_{ij}}{r_{ij}^6} + \frac{q_i q_j}{r_{ij}} \right] \quad (6)$$

This model has already been parametrized by de Andrade et al. for the simulation of other room-temperature ionic liquids involving 1-ethyl-3-methylimidazolium cations,^{15,16} EMI-AlCl₄ and EMI-BF₄, and correctly describes both structure and dynamics of the liquids. Using the histidine amino acid parameters, which also consists of an imidazolium ring, the authors derived a complete set of parameters for the bonds, angles, dihedrals, and van der Waals interactions. We used the same values in this study, and all of them are summarized in Tables 1–4.

These authors also obtained an electronic charge distribution of the cation from quantum mechanics calculations on the ab initio level using the one-conformation two-stage standard RESP fitting procedure.¹⁷ All of the corresponding atomic partial charges are reproduced in Figure 1.

TABLE 1: Bond Stretching Potential Parameters

bond	K_r (kJ mol ⁻¹ Å ⁻²)	r_{eq} (Å)
CT–CT	1297.04	1.526
CT–H1	1422.56	1.090
CT–HC	1422.56	1.090
CT–NA	1410.01	1.475
CR–H5	1535.53	1.080
CR–NA	1995.77	1.343
CW–H4	1535.53	1.080
CW–NA	1786.57	1.381
CW–CW	2297.02	1.350

TABLE 2: Bond Angle Potential Parameters

angle	K_θ (kJ mol ⁻¹ rad ⁻²)	θ_{eq} (deg)
H1–CT–H1	146.44	109.5
H1–CT–NA	209.20	109.5
CR–NA–CT	292.88	128.8
CW–NA–CT	292.88	121.2
CW–CW–NA	292.88	121.2
CW–CW–H4	146.44	119.7
CT–CT–H1	209.20	109.5
CT–CT–HC	209.20	109.5
HC–CT–HC	146.44	109.5
CT–CT–NA	209.20	109.5
NA–CR–NA	292.88	120.0
NA–CR–H5	146.44	120.0
CR–NA–CW	292.88	120.0
NA–CW–H4	146.44	120.0

TABLE 3: Dihedral Torsion Potential Parameters

torsion	V_n (kJ mol ⁻¹)	γ (deg)	n
proper torsions			
NA–CR–NA–CT	7.1128	180	2
H5–CR–NA–CT	7.1128	180	2
H5–CR–NA–CW	9.7278	180	2
NA–CR–NA–CW	9.7278	180	2
X–CT–CT–X	0.6508	0	3
X–CT–NA–X	0	0	2
X–CW–CW–X	27.8236	180	2
CW–CW–NA–CR	7.7404	180	2
CW–CW–NA–CT	7.7404	180	2
H4–CW–NA–CR	6.2760	180	2
H4–CW–NA–CT	7.7404	180	2
improper torsions			
X–X–CR–H5	4.6024	180	2
X–X–CW–H4	4.6024	180	2
X–X–CT–NA	4.1840	180	2

TABLE 4: Nonbonded van der Waals Potential Parameters

atom type	σ_{ii} (Å)	ϵ_{ii} (kJ mol ⁻¹)
HC	2.6495	0.0657
H1	2.4714	0.0657
H4	2.5106	0.0628
H5	2.4215	0.0628
CT	3.3997	0.4577
CR	3.3997	0.3598
CW	3.3997	0.3598
NA	3.2500	0.7113
F	3.1181	0.25522

Several other models for imidazolium cations have been developed in recent years. Among them, the one by Hanke et al. is of particular interest as they successfully calculated structural and dynamic properties of pure imidazolium salts¹⁸ and of their mixtures with water.¹⁹ In this model the imidazolium ring is kept rigid, and all the distance bonds are kept constant. But we preferred to allow for more degrees of freedom in our system, which is why we chose de Andrade's potential.

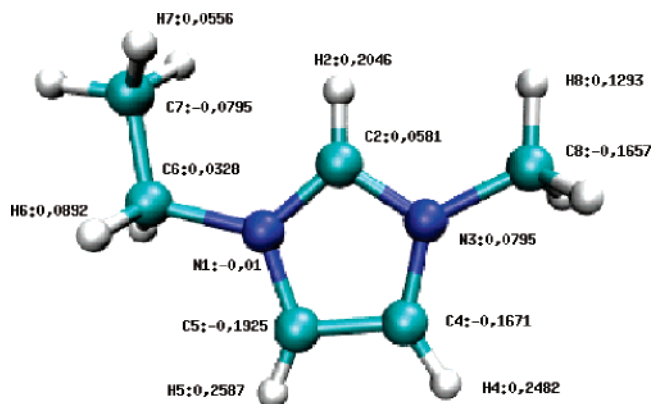


Figure 1. Atom types and corresponding partial charges of the imidazolium cation.

2.1.3. Intermolecular Potentials. Van der Waals interactions between all fluorine atoms (i.e., fluoride anions and fluorines in HF molecules) and imidazolium cations were also introduced using the AMBER force field. Fluorine parameters are also listed in Table 4.

Interactions between fluorides and HF molecules are a crucial point of this model. We chose to describe them by only one pair potential between anions and hydrogen atoms. This one has the same analytic formula as the H–F interaction in the HF3 model. This representation's greatest advantage is that it was formerly built to account for hydrogen bonds in liquid HF. In a former study of $\text{KF} \cdot 2\text{HF}$,^{8,9} the same model proved to be efficient in forming the various polyfluoride species in realistic proportions.

2.2. Computational Details. The MD simulations were performed using DLPOLY,²⁰ version 2.14, which was modified to introduce the HF3 potential. We used the Verlet algorithm with a time step of 1 fs to integrate the equations of motion.

The simulation box was built from the structure data obtained by Matsumoto et al. for the solid EMIF–HF,²¹ which was used as a starting point. HF molecules were added into the cell to obtain the correct proportion for the simulation of liquid EMIF·2.3HF. We used an orthorhombic box ($a = 37.0331$ Å, $b = 37.1957$ Å, and $c = 41.7108$ Å), containing 192 EMI^+ and F^- ions and 440 HF molecules, i.e., 5160 atoms, to reproduce the experimental² density of the melt of 1.13 g cm^{-3} at 298 K. The process of equilibration consisted in 200 ps simulations at temperatures growing from 2 to 298 K, in five steps. Then a 1 ns simulation was run at a 298 K temperature in the NVE ensemble. A cutoff radius of 16 Å was used for the calculation of short-range interactions, while the long-range electrostatic interactions were treated using the Ewald summation method.²²

3. Results and Discussion

3.1. Polyfluoride Anions. Very little is known about the polyfluoride anions $\text{F}(\text{HF})_n^-$ in the liquid state, although they have been very well characterized in solids as the $\text{KF} \cdot x\text{HF}$ crystals.

The only evidence for their existence in the liquid state is given by IR spectroscopy. For example, EMIF·2.3HF spectra show that there are not any free HF molecules in the liquid state, and several polyfluoride species have been identified with the help of ab initio calculations on these anions. Shodai et al., studying tetraalkylammonium fluorohydrogenates¹¹ ($\text{NR}_4\text{F} \cdot x\text{HF}$), and Hagiwara et al. in EMIF·2.3HF¹² concluded that the only existing species were $\text{F}(\text{HF})^-$, $\text{F}(\text{HF})_2^-$, and $\text{F}(\text{HF})_3^-$.

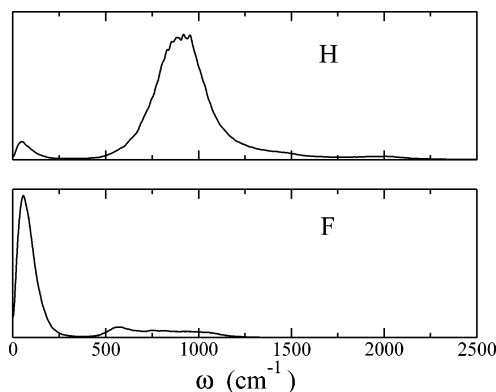


Figure 2. Vibrational power spectra, $f(\omega)$, obtained from the velocity autocorrelation functions for HF hydrogen atoms (top) and for all fluorine atoms (bottom).

Formation of higher polyfluorides ($n > 3$) should not occur since HF exists as a free molecule in $\text{NR}_4\text{F} \cdot x\text{HF}$ for values of x greater than 3.

Our results are consistent with these experimental facts as fluoride anions and HF molecules took exclusively the form of polyfluorides during the simulations. At equilibrium, the only existing species were $\text{F}(\text{HF})^-$, $\text{F}(\text{HF})_2^-$, and $\text{F}(\text{HF})_3^-$ with respective proportions of approximately 10%, 40%, and 50%. An HF molecule is considered bonded to a given fluoride ion if the distance between the hydrogen atom and the fluoride ion is smaller than a cutoff value of 2.1 Å, as in our previous studies. This cutoff distance arises from $g(r)$. These proportions seem quite realistic. We would like to underline that there is currently no quantitative way to investigate experimentally these proportions to confirm or deny these results. In principle NMR allows characterization and population analysis of the various polyfluorides, as shown by Shenderovich et al.²³ in a dispersed phase. But in the concentrated liquid, rapid exchange of HF molecules between polyfluoride anions causes the signals of the different complexes to overlap, due to the lack of time resolution. Nevertheless, “chemical common sense” suggests that $(\text{HF})_n\text{F}^- / (\text{HF})_m\text{F}^-$ with $n > m$ increases with HF proportion, as soon as $(\text{HF})_n\text{F}^-$ and $(\text{HF})_m\text{F}^-$ exist.

The only system containing polyfluoride species that had already been simulated by molecular dynamics is the $\text{KF} \cdot 2\text{HF}$ melt. In their ab initio molecular dynamics study,⁷ von Rosenvinge et al. computed the vibrational power spectra of all the atoms and managed to identify contributions from different polyfluorides in the H power spectra. The same calculation has been done in the present case, and Figure 2 gives the power spectra of F and H atoms, while Figure 3 displays the power spectra of H atoms involved in the three polyfluoride species formed. A comparison of the spectra obtained here and in the $\text{KF} \cdot 2\text{HF}$ study shows that there is a surprisingly good agreement, even though the methods and models used to obtain them are completely different. Most of the differences occur in the high ω values, i.e., above 1300 cm^{-1} . As shown by von Rosenvinge et al., intensity in this range of the power spectra is mostly due to the vibration of the hydrogen along the F–F axis. We can therefore attribute the observed discrepancy to the rigidity of HF molecules in our model. Furthermore the agreement considering the larger peak (around 1000 cm^{-1} , which mostly describes the rotation of hydrogen atoms around the F–F axis) improves from $\text{F}(\text{HF})^-$ to $\text{F}(\text{HF})_3^-$. This is expected since in the bifluoride anion $\text{F}(\text{HF})^-$ the proton is located at an equal distance (1.17 Å) from each fluorine atom, whereas in our study we obtained two different distances of

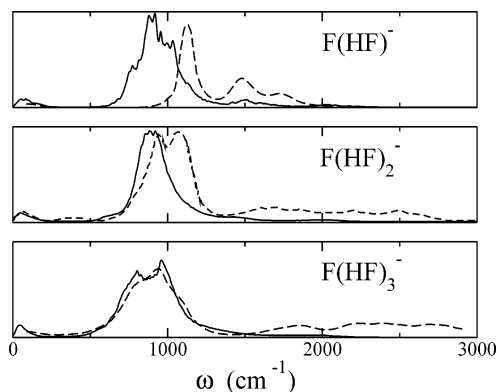


Figure 3. Vibrational power spectra, $f(\omega)$, obtained for the various polyfluoride species (solid line, present study; dashed line, ab initio molecular dynamics⁷ of $\text{KF} \cdot 2\text{HF}$).

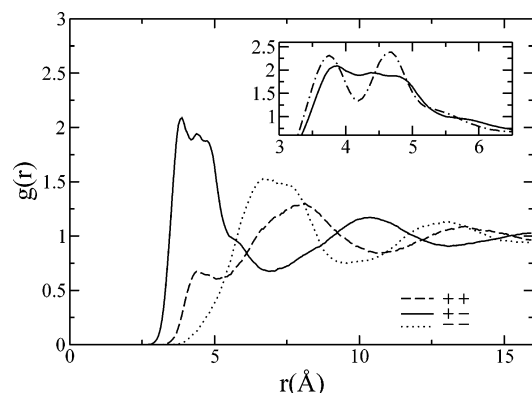


Figure 4. Self and cross radial distribution functions between imidazolium ring centers and fluoride anion (solid line, imidazolium–fluoride; dashed, imidazolium–imidazolium; dotted, fluoride–fluoride). The frame in the right top corner displays a detailed view of the first EMI^+F^- correlation peak with two different definitions of the ring center (solid line, C center; dashed–dotted line, C' center).

0.91 Å (as fixed in the HF3 model) and 1.48 Å. With the same F–H distance the geometry obtained for $\text{F}(\text{HF})_3^-$ agrees much better with the ab initio simulation where distances are, respectively, 1.00 and 1.48 Å.

3.2. Structural Features of Cations. **3.2.1. Cation–Anion Shells.** A first insight into the structure of the liquid is given by the radial distribution functions (RDFs). Figure 4 is a plot of such functions involving fluoride anions (i.e., the centers of the polyfluoride species) and the centers of mass C of the imidazolium ring. Their general shapes are typical of ionic liquids: The three RDFs reach extrema almost at the same distances (~ 3.5 – 7.0 – 10.5 – 13.5 Å), both self-terms being maximum when the cross term is minimum and vice versa. This denotes alternating cationic and anionic shells. The first peak of the EMI^+F^- RDF is larger than 1.5 Å and seems to have a substructure. This lead us to introduce C', the middle of the N1–N3 segment and recompute the RDF using it as the center of EMI^+ . The RDF then exhibits a splitted first peak as shown in the inset of Figure 4. This shows that all positions in the first solvation shell are not equivalent. A three-dimensional plot of the distribution of fluorides and imidazoliums around a given imidazolium is necessary to know where are privileged positions in the first solvation shell. Figure 5, on which the surfaces correspond to a fluoride density 9 times higher than the average density, clearly shows that the fluoride anions have a really sharp distribution around the ring hydrogen atoms. This explains the two peaks of the radial distribution function since those hydrogen atoms are not equally distant to the defined center of

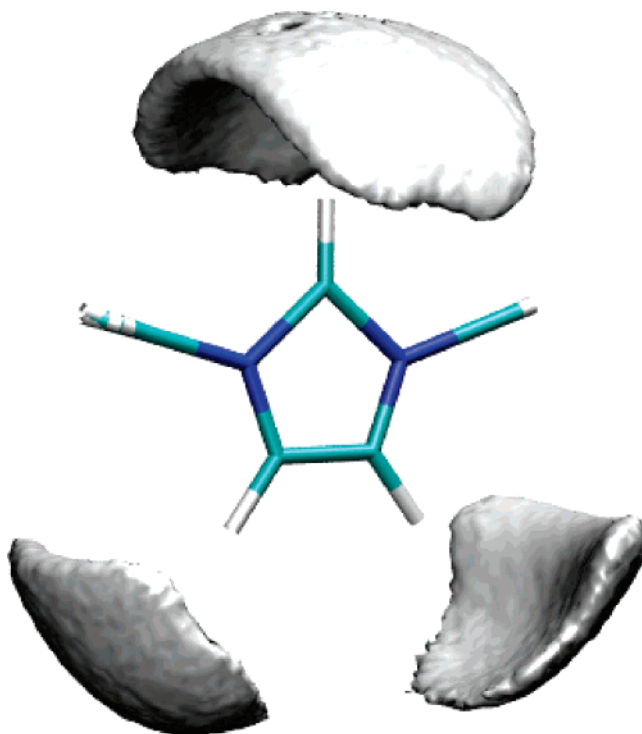


Figure 5. Three-dimensional density of fluoride anions around imidazolium. The surfaces are shown correspond to a density 9 times higher than the average density.

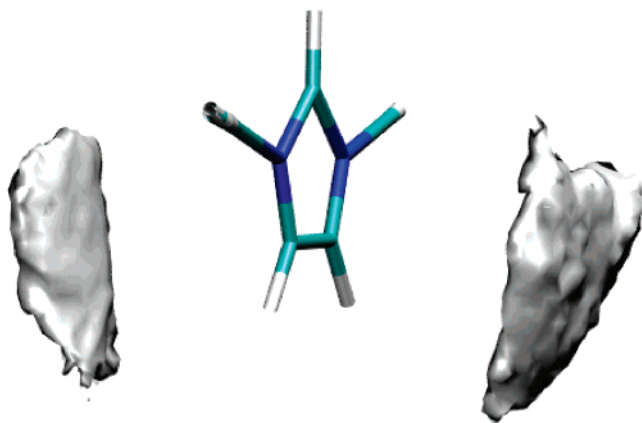


Figure 6. Three-dimensional density of the imidazolium cation's ring centers around a given imidazolium. The surfaces shown correspond to a density 3 times higher than the average density.

the ring. The same kind of distribution has been obtained by del Pópolo et al. in an ab initio simulation of liquid dimethylimidazolium chloride²⁴ (DMICl), whereas Voth et al. only observed it around the H2 atom in their study of 1-ethyl-3-methylimidazolium nitrate.²⁵ In the next section we will focus more precisely on the interaction between the ring hydrogen atoms and the fluoride anions.

Concerning imidazolium cations, Figure 4 only gives information on the distance between two of them. The RDF shows that the minimal cation–cation distance is 3.3 Å but that most of the cations are at distances of 4–10 Å from each other. To determine if a cation's first neighbor has a privileged position around it, Figure 6 shows the three-dimensional plot of imidazolium distribution. (Here the surfaces correspond to a density 3 times higher than the average one.) This suggests the existence of a partially stacked structure in this liquid, already pointed out by Hagiwara et al. in their X-ray diffraction study,²⁶ and is even more explicit in Figure 7. In this later representation,

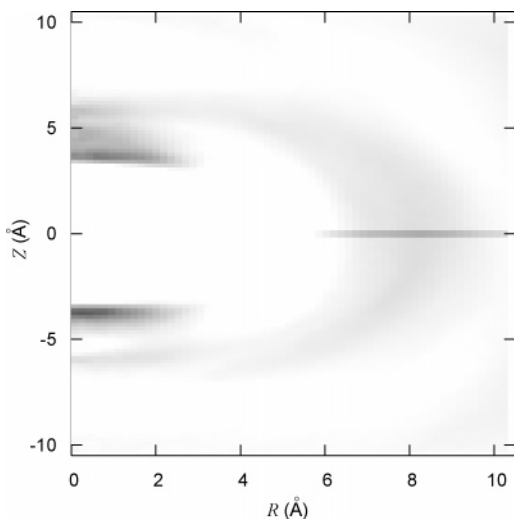


Figure 7. Two-dimensional density of imidazolium cation's ring centers around a given imidazolium. The origin is the imidazolium ring center, the O_z axis is perpendicular to the ring, and R is the radial distance to this axis. The darkest points correspond to a density 4 times higher than the average density, and white points correspond to a density lower than the average.

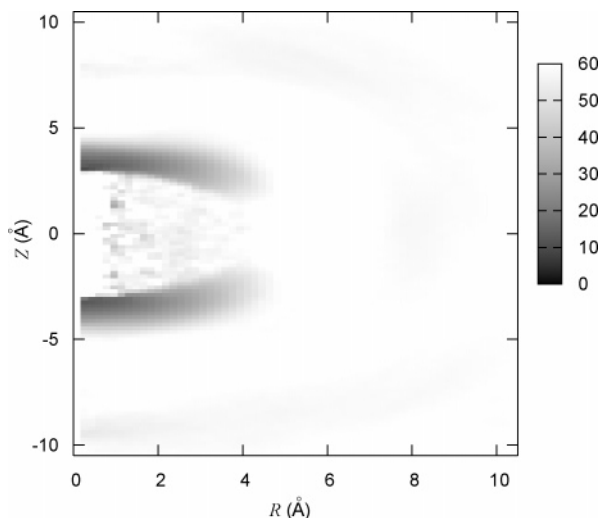


Figure 8. Two-dimensional plot of the mean value for the angle formed by two ring planes. In the close neighborhood of the ring center, dark points revealing fluctuations are due to a lack of statistical data.

Z is the distance from the center of an imidazolium ring, the (O_z) axis being perpendicular to the plane formed by the ring, whereas R is the radial distance to this (O_z) axis. Furthermore, this figure shows that the layered structure is partially conserved since the density of cations in the reference cation plane ($Z = 0$) is quite high.

To demonstrate the existence of stacks and layers of cations, the positional order pointed out is not fully sufficient: One has also to consider the orientational order. Then we calculated the mean value of the angle formed by two imidazolium rings at each point of the space. The result is shown in Figure 8 where we can see that this angle is of 0 – 20° in the higher-density region. This supports the previous conclusion about stacks. Concerning the neighbor in the same plane, no particular orientation can be revealed (as the mean value is the “magic angle”, i.e., 57.4° in this region of space), showing that the layered structure is not fully conserved, even in the short range.

3.2.2. Hydrogen Bonding. In solid EMIF–HF, hydrogen bonds are known to be formed between the imidazolium ring

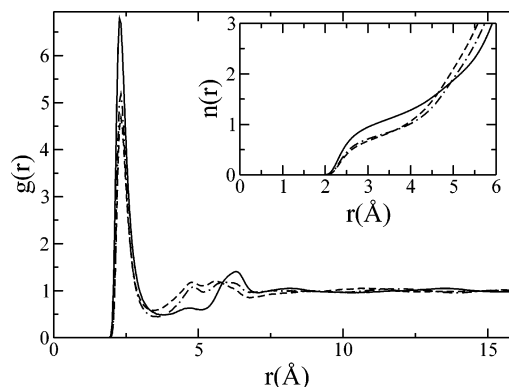


Figure 9. Radial distribution functions between imidazolium ring hydrogens and fluoride anion (solid line, F–H2; dashed, F–H4; dot-dashed, F–H5). The inset shows the corresponding running coordination numbers.

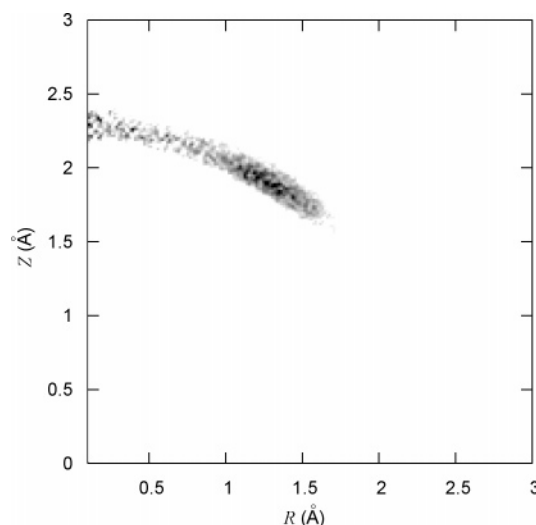


Figure 10. Fluoride presence around the C4–H4 axis. The origin is the H4 atom, O_z axis is the C4–H4 axis, and R is the radial distance to this axis. The higher density is clearly out of the axis.

hydrogen atoms and the fluoride anions,²¹ and X-ray spectroscopy experiments showed that in this compound the $H\cdots F$ bond distance is 1.951 Å for H2, 2.166 Å for H4, and 2.226 Å for H5. In liquid DMICl, hydrogen bonding also concerns the ring protons and the chloride anion, but in EMIF·2.3 HF such bonds are not observed experimentally,²¹ which is quite surprising. On the basis of Figure 5, it is clear that in the liquid fluoride ions still remain in the vicinity of these three hydrogen atoms. To determine if the resulting $H\cdots F$ interactions can be classified into hydrogen bonds, we considered two criteria: first, the distance between those pairs of atoms, and second, the directionality of the interaction.

Figure 9 is a plot of the RDF for fluorine anions and imidazolium ring protons. All of them are characterized by a sharp peak at 2.2 Å . The inset of this figure shows that all of the running coordination numbers are 1 after the first peak, so that there is one fluoride anion surrounding each hydrogen. Similar RDFs have already been obtained for ab initio simulations of DMICl.²⁴ As DMICl is known to form hydrogen bonds, one would be tempted to conclude the same for EMIF·2.3HF.

But the second criteria is directionality. The plot of probability of fluoride anion presence around the C–H axis of the imidazolium rings is given in Figure 10 for C4. In this figure, Z is the distance along the C4–H4 axis while the origin is the H4 atom. It shows that the fluoride privileged position is not in

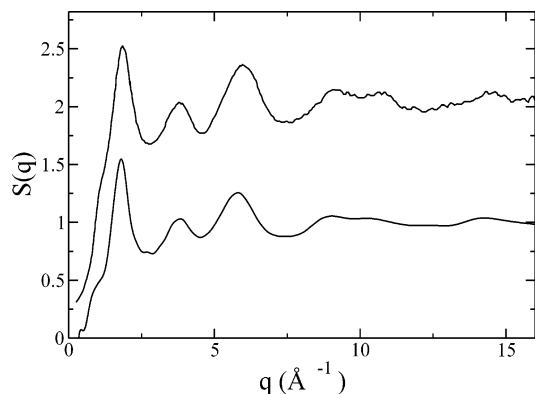


Figure 11. Total structure factor as obtained from our calculations and from experiments.²⁶ The experimental curve is displaced upward by 1.

the C4–H4 direction so that the H–F interaction cannot be classified as a hydrogen bond, contrary to DMICl.²⁴ Identical results have been obtained for H2 and H5. Our computations, in agreement with experimental results, suggest that there is no hydrogen bonding in this liquid.²¹

3.3. Comparison with Diffraction Data. The partial structure factors for each pair of atoms were calculated from our molecular dynamics simulations using the formula

$$S_{\alpha\beta}(q) = \delta_{\alpha\beta} + \int_0^{r_{\text{cut}}} r^2 \frac{\sin(qr)}{qr} (g_{\alpha\beta} - 1) dr \quad (7)$$

Since the r_{cut} used was large (16 Å), errors due to truncation of the integral should concern very small q values only. Then we could calculate the total structure factor by

$$S(q) = \frac{1}{\sum_{\alpha} (f_{\alpha}(q))^2 N_{\alpha}} \sum_{\alpha, \beta} f_{\alpha}(q) f_{\beta}(q) \sqrt{N_{\alpha} N_{\beta}} S_{\alpha\beta}(q) \quad (8)$$

where f_{α} is the atomic form factor of atom α and was calculated using its analytical approximation

$$f_{\alpha}(q) = c_{\alpha} + \sum_{i=1}^4 a_{\alpha,i} \exp\left(-b_{\alpha,i} \left(\frac{q}{4\pi}\right)^2\right) \quad (9)$$

in which all $a_{\alpha,i}$, $b_{\alpha,i}$, and c_{α} were taken from the international tables for X-ray spectroscopy.²⁷

Figure 11 provides this structural data as obtained by our simulations and by X-ray experiments reproduced from ref. 26.

One can see a very good agreement between both curves, showing that the structure is well reproduced by our model. Hagiwara et al. tried to attribute the first sharp diffraction peak. To do so, they compared their obtained spectra with the one of solid EMIF–HF. They found out that this peak, which is at a q value of 1.85 Å^{−1}, corresponds to the biggest peak in the solid spectra. As EMIF–HF shows a layered structure, with an interlayer distance of 3.38 Å, the authors attributed this peak to a partial preservation of the layered structure in the liquid. Even though this assumption is in partial agreement with our spatial distribution functions, i.e., preservation of stacks of cations, a further examination of the corresponding radial distribution function in Figure 4 shows that the mean distance between two neighboring cations is much greater, above 4 Å (Figure 4, dashed line). To examine more precisely the shape of the total structure factor and to determine the origins of the main peaks, we calculated the partial structure factors of

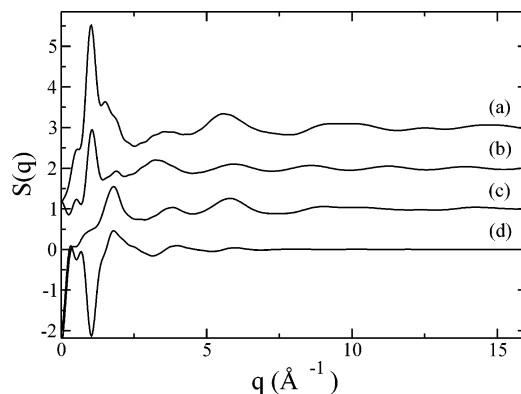


Figure 12. Total structure factor (c) and its decomposition in partial structure factors for: imidazolium cations (a), polyfluoride anions (b), and the cross term imidazolium–polyfluoride (d). Part a was shifted by 2, and part b was shifted by 1.

imidazolium cations, polyfluoride anions, and their cross term to quantify all of their contributions. The following formulas were used

$$S_{++}(q) = \frac{1}{\sum_{\alpha \in \text{imid}} (f_{\alpha}(q))^2 N_{\alpha}} \sum_{\alpha, \beta \in \text{imid}} f_{\alpha}(q) f_{\beta}(q) \sqrt{N_{\alpha} N_{\beta}} S_{\alpha\beta}(q) \quad (10)$$

$$S_{--}(q) = \frac{1}{\sum_{\alpha \in \text{polyf}} (f_{\alpha}(q))^2 N_{\alpha}} \sum_{\alpha, \beta \in \text{polyf}} f_{\alpha}(q) f_{\beta}(q) \sqrt{N_{\alpha} N_{\beta}} S_{\alpha\beta}(q) \quad (11)$$

$$S_{+-}(q) = \frac{1}{\sum_{\alpha} (f_{\alpha}(q))^2 N_{\alpha}} \sum_{\alpha \in \text{imid}, \beta \in \text{polyf}} f_{\alpha}(q) f_{\beta}(q) \sqrt{N_{\alpha} N_{\beta}} S_{\alpha\beta}(q) \quad (12)$$

The resulting curves are displayed in Figure 12. From this plot, one first can see that the two self-terms are characterized by a high peak at 1 Å^{−1} that can easily be differentiated from the first sharp diffraction peak at 1.85 Å^{−1}. They are counterbalanced by a deep negative peak in the cross term. Consequently, in the resulting total structure factor, there is no peak but a small shoulder at $q = 1$ Å^{−1}. Then the examination of the curves around this first sharp diffraction peak at around 1.85 Å^{−1} shows that it is mostly due to the distance between cations and polyfluoride anions. This was strongly suggested by the corresponding radial distribution function, as shown in Figure 4. As expected the oscillations at high q values are only due to the inter-imidazolium and inter-polyfluoride partial structure factors since they correspond to intramolecular structural features.

4. Conclusion

We have shown in this study that it is possible to use classical but efficient potentials to model a complex ionic liquid, composed of a mixture of ionic species with hydrogen fluoride molecules. The structure of the simulated liquid matches very well with experimental results.

This model also yields the formation of polyfluoride species composed of a central fluoride anion surrounded by 1, 2, or 3 HF molecules, which is consistent with IR spectroscopy data and ab initio studies. The model is therefore validated by several features of the structure. An important dynamical property of those clusters, the vibrational power spectra, is also given.

Hagiwara et al. experimentally demonstrated that some structures existing in the crystal remain in the liquid state. Our simulations confirm this for the short-range stacking of cations, but there is no evidence for layers. The previous authors also revealed the absence of hydrogen bonds between imidazolium and fluoride ions. This property is rather surprising considering similar other systems forming such hydrogen bonds (DMICl, solid EMIF–HF). Nevertheless, this result is clearly supported by the present study.

Furthermore, experimental X-ray diffraction spectra are quite well reproduced by our model. The use of simulation allows deeper insight to the partial contributions to these data.

Further work should include more dynamical aspects of this liquid. Transport properties are of particular interest for the practical application of this system. More specifically, it would be valuable to separate the different contributions of the various polyfluoride species to these properties.

References and Notes

- (1) Hagiwara, R.; Hirashige, T.; Tsuda, T.; Ito, Y. *J. Fluorine Chem.* **1999**, *99*, 1.
- (2) Hagiwara, R.; Hirashige, T.; Tsuda, T.; Ito, Y. *J. Electrochem. Soc.* **2002**, *149*, D1.
- (3) Tsuda, T.; Nohira, T.; Nakamori, Y.; Matsumoto, K.; Hagiwara, R.; Ito, Y. *Solid State Ionics* **2002**, *149*, 295.
- (4) Me, U.; Takeda, M.; Toriumi, A.; Kominato, A.; Hagiwara, R.; Ito, Y. *J. Electrochem. Soc.* **2003**, *150*, A499.
- (5) Yoshino, H.; Nomura, K.; Matsubara, S.; Oshima, K.; Matsumoto, K.; Hagiwara, R.; Ito, Y. *J. Fluorine Chem.* **2004**, *125*, 1127.
- (6) Yoshino, H.; Matsubara, S.; Oshima, K.; Matsumoto, K.; Hagiwara, R.; Ito, Y. *J. Fluorine Chem.* **2004**, *125*, 455.
- (7) von Rosenvinge, T.; Parrinello, M.; Klein, M. L. *J. Chem. Phys.* **1997**, *107*, 8012.
- (8) Simon, C.; Cartailier, T.; Turq, P. *Phys. Chem. Chem. Phys.* **2001**, *3*, 3119.
- (9) Simon, C.; Cartailier, T.; Turq, P. *J. Chem. Phys.* **2002**, *117*, 3772.
- (10) Hagiwara, R.; Matsumoto, K.; Nakamori, Y.; Tsuda, T.; Ito, Y.; Matsumoto, H.; Momota, K. *J. Electrochem. Soc.* **2003**, *150*, D195.
- (11) Shodai, Y.; Kohara, S.; Ohishi, Y.; Inaba, M.; Tasaka, A. *J. Phys. Chem. A* **2004**, *108*, 1127.
- (12) Hagiwara, R.; Nakamori, Y.; Matsumoto, K.; Ito, Y. *J. Phys. Chem. B* **2005**, *109*, 5445.
- (13) Klein, M. L.; McDonald, I. R. *J. Chem. Phys.* **1979**, *71*, 298.
- (14) Cornell, W. D.; Cieplak, P.; Bayly, C. I.; Gould, I. R.; Merz, K. M.; Ferguson, D. M.; Spellmeyer, D. C.; Fox, T.; Caldwell, J. W.; Kollman, P. A. *J. Am. Chem. Soc.* **1995**, *117*, 5179.
- (15) de Andrade, J.; Boes, E.; Stassen, H. *J. Phys. Chem. B* **2002**, *106*, 3546.
- (16) de Andrade, J.; Boes, E.; Stassen, H. *J. Phys. Chem. B* **2002**, *106*, 13344.
- (17) Bayly, C. I.; Cieplak, P.; Cornell, W. D.; Kollman, P. A. *J. Phys. Chem.* **1993**, *97*, 10269.
- (18) Hanke, C. G.; Price, S. L.; Lynden-Bell, R. M. *Mol. Phys.* **2001**, *99*, 801.
- (19) Hanke, C. G.; Lynden-Bell, R. M. *J. Phys. Chem. B* **2003**, *107*, 10873.
- (20) Forester, T. R.; Smith, W. DLPOLY Program, 1995. <http://www.dl.ac.uk/TCS/Software/DLPOLY/>.
- (21) Matsumoto, K.; Tsuda, T.; Hagiwara, R.; Ito, Y.; Tamada, O. *Solid State Sci.* **2002**, *4*, 23.
- (22) Ewald, P. *Ann. Phys.* **1921**, *36*, 253.
- (23) Shenderovich, I.; Smirnov, S.; Denisov, G.; Gindin, V.; Golubev, N.; Dunger, A.; Reibke, R.; Kirpekar, S.; Malkina, L.; Limbach, H. H. *Ber. Bunsen-Ges. Phys. Chem.* **1998**, *102*, 422.
- (24) Pópolo, M. G. D.; Lynden-Bell, R. M.; Kohanoff, G. *J. Phys. Chem. B* **2005**, *109*, 5895.
- (25) Pópolo, M. G. D.; Voth, G. A. *J. Phys. Chem. B* **2004**, *108*, 1744.
- (26) Hagiwara, R.; Matsumoto, K.; Tsuda, T.; Ito, Y.; Kohara, S.; Suzuya, K.; Matsumoto, H.; Miyazaki, Y. *J. Non-Cryst. Solids* **2002**, *312–314*, 414.
- (27) *International Tables for X-ray Crystallography*; International Union of Crystallography: Birmingham, U. K., 1968–1974.